Accepted Manuscript

Interfacial reactions in Sn/Bi_2Te_3, Sn/Bi_2Se_3 and $Sn/Bi_2(Te_{1-x}Se_x)_3$ couples

Sinn-wen Chen, Chih-yu Wu, Hsin-jay Wu, Wan-ting Chiu

PII: S0925-8388(14)01224-9
DOI: http://dx.doi.org/10.1016/j.jallcom.2014.05.127
Reference: JALCOM 31316

To appear in:

Received Date: 29 October 2013
Revised Date: 17 May 2014
Accepted Date: 19 May 2014

Please cite this article as: S-w. Chen, C-y. Wu, H-j. Wu, W-t. Chiu, Interfacial reactions in Sn/Bi_2Te_3, Sn/Bi_2Se_3 and $Sn/Bi_2(Te_{1-x}Se_x)_3$ couples, (2014), doi: http://dx.doi.org/10.1016/j.jallcom.2014.05.127

Interfacial reactions in Sn/Bi_2Te_3, Sn/Bi_2Se_3 and Sn/$Bi_2(Te_{1-x}Se_x)_3$ couples

[*]Sinn-wen Chen, Chih-yu Wu, Hsin-jay Wu, and Wan-ting Chiu

Department of Chemical Engineering, National Tsing Hua University

Abstract

$Bi_2(Te_{1-x}Se_x)_3$ is an important kind of n-type thermoelectric material. In this study, interfacial reactions at 250℃ in the Sn/Bi_2Te_3, Sn/Bi_2Se_3 and Sn/$Bi_2(Te_{1-x}Se_x)_3$ couples are examined. In the Sn/Bi_2Te_3 couple, the reaction zone is found to be non-planar and the reaction path is liquid/(liquid+SnTe)/Bi_2Te_3. But with only 2.0 at.%Se addition to the Bi_2Te_3 substrate, very different reaction results are observed. In the Sn/$Bi_2(Te_{1-x}Se_x)_3$ couple, the reaction layers are planar, and the reaction path is liquid/SnTe/$BiTe_x$/ $Bi_2(Te_{1-x}Se_x)_3$. In the Sn/Bi_2Se_3 couple, the reaction layers are also planar, the reaction path is liquid/SnSe/BiSe/Bi_2Se_3, and the Bi content in the SnSe phase varies. The growth rates in the Sn/Bi_2Te_3 couples are very fast, and the reaction layer is as thick as 1174 μm in just 15 minutes. Very dramatic reduction of growth rates has been observed with Se addition to the substrates, and the reaction layer is only 9 μm in the Sn/$Bi_2(Te_{2.9}Se_{0.1})$ couples after reaction for 30 minutes.

Key words: $Bi_2(Te_{1-x}Se_x)_3$, Interfacial reaction, Thermoelectric

[*] Corresponding author: E-mail:swchen@mx.nthu.edu.tw; Tel: +886-3-5721734; Fax:+886-3-5715408

1. Introduction

Energy shortages are an increasingly critical challenge. Thus, inspired mostly by power generation from waste heat and cooling with more compact solid state coolers based on the Seebeck and Peltier effects [1-5], thermoelectric devices have attracted intensive study. Over the past 10 years, from 2003 to 2012, there were 483 American patents and 6421 publications with the title word "thermoelectric" listed in the Web of Science database. Among various kinds of thermoelectric materials, the p-type Bi_2Te_3 with Sb_2Te_3, and the n-type Bi_2Te_3 with Bi_2Se_3 are the earliest and most popularly used commercial thermoelectric materials [1-15].

There are a series of p-n junction units and numerous joints in thermoelectric devices, and the quality of these joints is crucial to the properties of devices. However, there are few studies related to joining [6-15]. Sn-based solders are often used in Bi_2Te_3-based devices. Although barrier layers exist between solders and thermoelectric materials, it has been reported that the Sn might penetrate and react with thermoelectric materials [6,7], so it is fundamentally important to examine their interfacial reactions. This study investigates the interfacial reactions between Sn and the n-type $Bi_2(Te_{1-x}Se_x)_3$ and provides information not previously available in the literature.

2. Experimental procedures

Thermoelectric material substrates, Bi_2Te_3, Bi_2Se_3, and $Bi_2(Te_{1-x}Se_x)_3$ were prepared with pure Bi shots (99.9 wt.%, Admat Midas, Norristown, PA), Te shots (99.99 wt.%, Alfa Aesar, Ward Hill, MA), and Se shots (99.999 wt.%, Alfa Aesar, Ward Hill, MA). Proper amounts of pure constituent elements were weighed and encapsulated in a quartz tube at 10^{-2} torr.

The sample capsule was first heated up to 500℃ for 6 hours, 700℃ for another 18 hours, and then quenched in air. The quenched sample capsules were annealed at 550℃ to homogenize the thermoelectric ingots. After one week, the capsules were removed from the furnace. The ingots were removed from the quartz tubes and cut into 2 mm-thick pieces of substrates.

The thermoelectric substrates were encapsulated with pure Sn shots (99.99 wt.%, Alfa Aesar, Ward Hill, MA) at 10^{-2} torr, and the sample capsules were placed at 250 ℃ until the Sn shots became molten. Liquid Sn surrounded the thermoelectric substrates, and a liquid (molten Sn)/solid thermoelectric substrate [Bi_2Te_3, Bi_2Se_3, and $Bi_2(Te_{1-x}Se_x)_3$] couple was formed. After predetermined lengths of reaction time, the sample capsules were removed from the furnace and quenched in air.

Reacted couples were then removed from the quartz tubes, cut, mounted, and metallographically analyzed using scanning electron microscopy (SEM, Hitachi S-2500). Compositions of the reaction layers were determined using electron probe microanalysis (EPMA, JEOL, JXA 8200-SX). The accelerating voltage and beam current were at 12.0 kV and 15 nA, respectively. PbTe, Sn, Se and Bi were used as standards for the ZAF corrections [16] from intensities of Te Lα, Sn Lα, Se Lα and Bi Mα to concentrations. The spot size of the EPMA analysis is chosen to be smaller than the dimension of each reaction layer and the obtained composition is an averaged value of at least five times measurements; in general, the quantitative accuracy is about 0.1% for compositional analysis. Elemental mapping analysis is also conducted using the EPMA to highlight the distribution of the elements of the reaction layers. The reaction layer thickness was determined using a microscope equipped with an image analyzer (Image-Pro Plus, Media Cybernetics Inc.).

3. Experimental results and discussion

Sn/Bi_2Te_3 couples

Figure 1(a) is the BEI (back-scattered electron image) micrograph of the Sn/Bi_2Te_3 couple reacted at 250℃ for 5 minutes. Since Sn is molten at 250℃, the couple is a liquid Sn/solid Bi_2Te_3 couple. An irregular reaction zone is observed. It is also noted that the reaction zone is not a single phase region. Figures 1(b) and 1(c) show the results after reaction times of 10 minutes and 15 minutes, respectively. Similar microstructures are observed in these samples, and the reaction zones consist of various phases. As revealed in Figure 1(b), the reaction zone consists of at least two regions. The region near the Bi_2Te_3 substrate is brighter, and this brighter region has homogenously distributed fine bright spots. The region near the Sn side is darker but contains larger bright pieces of materials.

Figure 2(a) is the elemental mapping of the reaction zone in a 10-minute reacted sample, and Figure 2(b) is its SEI (secondary electron image) micrograph of the etched reaction zone. Compositional analysis indicates that the larger bright pieces in the reaction zone are unreacted Bi_2Te_3. The reacted microstructures are similar to those observed in Sn/Te, Sn-Bi/Te and related systems [8,10,15]. The reaction zone could consist of SnTe and liquid at 250℃, and the bright fine spots are Bi precipitates formed during solidification. The average EPMA-determined composition of the reaction zone near the Sn side is Sn-1.4 at.%Bi-35.1 at.%Te. This is in agreement with the presumption that reaction zone is a three phase mixture, Sn+Bi+SnTe. It should be mentioned that phase identification is conducted in this study only by compositional analysis together with the available related phase diagrams, and not confirmed by diffraction analysis.

Comparing the results from Sn/Te, Sn-Bi/Te and related systems [8,10,15], the following reaction mechanism is proposed. Molten Sn erodes and reacts with the Bi_2Te_3 substrate at a very fast rate, a porous SnTe phase is formed which is mixed with molten Sn, and excess Bi dissolves in molten Sn. This reaction-formed region is the brighter region as shown in Figure 1(b). Then Te moves toward the Sn side, and thus Te content is higher and Bi content is lower near the Sn side. The reaction path is liquid/SnTe+liquid/Bi_2Te_3. When the sample is removed from the furnace, the liquid solidifies, and Sn and Bi phases are formed. Since molten Sn erodes the substrate quickly and irregularly, as shown in Figure 2(c), some tips of the unreacted Bi_2Te_3 substrates might be fragmented, taken from the substrates, and entrapped by the very fast-growing reaction zone. This region primarily formed during solidification is the darker region near the Sn phase.

As shown in Figures 1(a)-1(c), the reaction phases in the Sn/Bi_2Te_3 couples are similar for the reaction at 250℃ with various lengths of reaction time. As shown in Figure 3, the reaction layer grows thicker with longer reaction time, and the reaction rates are very fast. The reaction layer is as thick as 1174 μm after only 15 minutes reaction. Since the reaction zone is irregular, the thickness values shown are average results of at least three different measurements in order to have reliable data.

Sn/Bi_2Se_3 couples

Figure 4(a) is a BEI micrograph of the Sn/Bi_2Se_3 couple reacted at 250℃ for 10 minutes. A reaction zone is formed that is relatively planar compared to that in the Sn/Bi_2Te_3 couple, as mentioned above. Analysis of the reaction zone reveals that it consists of four different reaction phase regions: the dark layer, the gray layer, the bright layer, and the brightest spots. The micrographs of the couples reacted for 30 minutes, 60 minutes and 90 minutes are shown in Figures 4(b), 4(c) and 4(d), respectively. Similar results are observed in the Sn/Bi_2Se_3 couples reacted with various lengths of time, and as shown in Figure 3, the reaction zone is thicker with longer reaction time.

Figure 5 is the elemental mapping of the Sn/Bi_2Se_3 couple reacted at 250℃ for 90 minutes. There is a thin layer adjacent to the substrate, whose composition is Sn-51.5 at.%Bi-47.5 at.%Se, and is the BiSe phase [17]. Sn and Se are the faster moving species, while Bi is slowest [18]. Sn diffuses toward the substrate, Se diffuses toward the Sn side, and the relatively immobile Bi is left behind, so a Bi-rich layer is created.

Although there are variations, the concentrations of Se in the reaction zone are primarily divided into two regions. The gray one adjacent to the Bi_2Se_3 substrate has lower Se concentration, and is Sn-20.2 at.%Bi-33.1 at.%Se. That of the Se-rich region, i.e. the dark region in Figure 4(d), is Sn-0.4 at.%Bi-46.5 at.%Se. Both of these layers are the SnSe phase [19] although their Bi and Se contents are different. The compositional analysis indicates the brightest spots are the Bi phase, although the measured compositional values vary because the bright spots are small and their signals might be influenced by the background phase.

Figure 6 is the reaction path in the Sn/Bi_2Se_3 couple superimposed on the Sn-Se-Bi 250℃ phase equilibria isothermal section [20]. In the initial contact, part of the Bi_2Se_3 substrate is dissolved into the molten Sn. The liquid phase becomes a Sn-Se-Bi melt near the interface, and it is still pure Sn away from the interface. Sn and Se react to form the SnSe phase at the interface, and the Bi is dissolved in the liquid phase. As the reaction continues, Sn diffuses toward the substrate and the entire reaction zone is primarily the SnSe phase with different compositions. Se diffuses toward liquid side, and BiSe is formed adjacent to the Bi_2Se_3 phase. The reaction path at 250℃ is thus liquid/SnSe/BiSe/Bi_2Se_3. The liquid phase solidifies when the sample is removed from the furnace, and Sn and Bi phases are formed during solidification, as can be found near the Sn/reaction zone interface.

It should be noted that there are numerous undetermined compounds in the Bi-Se binary system [17], and BiSe has been reported as metastable compound in the literature [17,21]. Since most of the Bi-Se compounds have not actually been determined and identification of these phases is also not the primary research interest of this study, only Bi_2Se_3 and BiSe are considered in Figure 6.

Sn/$Bi_2(Te_{1-x}Se_x)_3$ couples

Figure 7(a) is a BEI micrograph of the Sn/$Bi_2(Te_{0.9}Se_{0.1})_3$ couple reacted at 250 ℃ for 10 minutes, and two reaction layers can be observed. Although only 6.0 at.%Se is introduced into the substrate, the morphology of the reaction zone has been changed significantly and is very different from those in the Sn/Bi_2Te_3 couples shown in Figures 1(a)-1(c). The composition of the dark layer is Sn-4.0 at.%Bi-43.8 at.%Te-2.2 at.%Se and it is the SnTe phase. The composition of the bright phase is Sn-53.4 at.%Bi-44.5 at.%Te-1.3 at.%Se, and it is the Bi_4Te_3 phase. The SnTe phase is a common reaction product in most of the Sn/Te (alloys) couples [8,10,12,14,15]. Similar to compounds in the Bi-Se binary system [17], there are numerous binary compounds in the Bi-Te binary system [22], and the Bi_4Te_3 phase has been reported as a metastable compound [22,23].

Micrographs of the couples reacted for 30, 60, 90 and 120 minutes are shown in Figures 7(b)-7(e). The reaction layers grow thicker with longer reaction time, as shown in Figure 3, and the reaction results are similar to those reacted for 10 minutes. The darker layer is the SnTe phase. However, a closer analysis of the brighter region of the reaction zone as shown in Figures 7(c)-7(e) reveals there are different layers in the brighter region. In addition to the Bi_4Te_3 layer, a light gray layer with composition of Bi-49.5 at.%Te-4.1 at.%Se is found and is identified as the BiTe phase. It has been reported that the numerous binary Bi-Te compounds are an infinitely adaptive series formed according to the $(Bi_2)_m(Bi_2Te_3)_n$ formula [24]. The reaction layers' identification as Bi_4Te_3 and BiTe phases are based on their compositional analysis results only. Since there are a series of undetermined compounds, these reaction phases could have evolved according to the reaction time as well, and the BiTe compound could be referred to as $BiTe_x$. The reaction path is liquid/SnTe/$BiTe_x$/$Bi_2(Te_{0.9}Se_{0.1})_3$.

Figures 8(a)-(c) are BEI micrographs of the Sn/$Bi_2(Te_{2.9}Se_{0.1})$ couples reacted at 250℃. Similar to those in the Sn/$Bi_2(Te_{0.9}Se_{0.1})_3$, the reaction layers are planar and the reaction products are SnTe and $BiTe_x$ phase, and the reaction path is liquid/SnTe/ $BiTe_x$/$Bi_2(Te_{2.9}Se_{0.1})$. The question of why a small amount of 2.0 at.%Se added to the Bi_2Te_3 substrate would completely alter the reaction results is interesting and needs to be examined in the future.

Reaction layer thicknesses for the Sn/Te [8], Sn/Bi_2Te_3, Sn/Bi_2Se_3, Sn/Sb_2Te_3 [15], Sn/$(Bi_{0.25}Sb_{0.75})_2Te_3$ [15] and Sn/$Bi_2(Te_{1-x}Se_x)_3$ couples reacted at 250℃ are shown in Figure 3. Since the reaction rates are very different, the Y-axis on the right-hand size is for the Sn/Te, Sn/Bi_2Te_3, Sn/Sb_2Te_3 and Sn/$(Bi_{0.25}Sb_{0.75})_2Te_3$, while that on the left-hand side is for the Sn/Bi_2Se_3 and Sn/$Bi_2(Te_{1-x}Se_x)_3$. It can be noted that, though the reaction rates are very fast for most of these couples, when a small amount of Se is added, the reaction rates are reduced dramatically. The reason for the change of reaction rates is likely related to the interfacial reaction phases and morphology and is definitely worthy of further investigations. Furthermore, the compounds formed at the interfaces and their different morphologies would have profound effects upon the properties of the thermoelectric joints and the devices, detail analyses and understanding are fundamentally important and need to be examined in the future.

4. Conclusions

Interfacial reactions at 250℃ in the Sn/Bi_2Te_3, Sn/Bi_2Se_3 and Sn/$Bi_2(Te_{1-x}Se_x)_3$ couples are examined. The reaction paths are liquid/(liquid+SnTe)/Bi_2Te_3 in the Sn/Bi_2Te_3 couple, liquid/SnSe/BiSe/Bi_2Se_3 in the Sn/Bi_2Se_3 couple, and liquid/SnTe/ $BiTe_x$/$Bi_2(Te_{1-x}Se_x)_3$ in the Sn/$Bi_2(Te_{1-x}Se_x)_3$ couple. With only 2.0 at.%Se addition to the Bi_2Te_3 substrate, very different morphologies and different reaction rates are observed. The reason for this dramatic change needs to be further examined in the future.

5. Acknowledgment

This study is financially sponsored by the National Science Council of Taiwan (NSC99-2221-E-007-093-MY3).

6. References

[1] G. Chen, M.S. Dresselhaus, G. Dresselhaus, J.-P. Fleurial and T. Caillat, Recent developments in thermoelectric materials, Int. Mater. Rev. 48 (1) (2003) 45-66.

[2] K. Rothe, M. Stordeur and H.S. Leipner, Power factor anisotropic of p-Type and n-Type conductive thermoelectric Bi-Sb-Te thin films, J. Electron. Mater. 39 (9) (2010) 1395-1398.

[3] A. Shakouri, Recent developments in semiconductor thermoelectric physics and materials, Annu. Rev. Mater. Res. 41 (2011) 399-431.

[4] N. Keawprak, S. Lao-ubol, C. Eamchotchawalit and Z.M. Sun, Thermoelectric properties of $Bi_2Se_xTe_{3-x}$ prepared by Bridgman method, J. Alloys and Comp. 509 (2011) 9296-9301.

[5] Y. Ma, W. Wijesekara and A.E.C. Palmqvist, Electrochemical deposition and characterization of thermoelectric ternary $(Bi_xSb_{1-x})_2Te_3$ and $Bi_2(Te_{1-y}Se_y)_3$ thin films, J. Electron. Mater. 41 (6) (2012) 1138-1146.

[6] M.M. Nanda, Joining Techniques for Bi_2Te_3 elements in thermoelectric cooling devices, Electrochem. Technol. 2 (1964) 134-137.

[7] D.D. Allred and O.V. Nguyen, Accelerated life test for thermoelectric junctions: solder element interactions, in: Proceedings of Seventh International Conference on Thermoelectric Energy Conversion, Arlington, TX, 1988, pp. 137-140.

[8] S.-W. Chen and C.-N. Chiu, Unusual cruciform pattern interfacial reactions in Sn/Te couples, Scr. Mater. 56 (2007) 97-99.

[9] L.W. da Silva and M. Kaviany, Micro-thermoelectric cooler: interfacial effects on thermal and electral transport, Int. J. Heat Mass Transfer 47 (2004) 2417-2435,.

[10] C.-N. Chiu, C.-H. Wang and S.-W. Chen, Interfacial reactions in the Sn-Bi/Te couples, J. Electron. Mater. 37 (1) (2007) 40-44.

[11] O.D. Iyore, T.H. Lee, R.P. Gupta, J.B. White, H.N. Alshareef, M.J. Kim and B.E. Gnade, Interface characterization of nickel contacts to bulk bismuth tellurium selenide, Surf. Interface Anal. 41 (2009) 440-444.

[12] Y.C. Lan, D.Z. Wang, G. Chen and Z.F. Ren, Diffusion of nickel and tin in p-type $(Bi,Sb)_2Te_3$ and n-type $Bi_2(Te,Se)_3$ thermoelectric materials, Appl. Phys. Lett. 92 (2008) 101910.

[13] N.-H. Bae, S. Han, K.E. Lee, B. Kim and S.-T. Kim, Diffusion at interfaces of micro thermoelectric devices, Curr. Appl. Phys. 11 (2011) S40-S44.

[14] T.Y. Lin, C.N. Laio and A.T. Wu, Evalution of diffusion barrier between Lead-free solder systems and thermoelectric materials, J. Electron. Mater. 41 (1) (2012) 153-158.

[15] S.-W. Chen, H.-J. Wu, C.-Y. Wu, C.-F. Chang and C.-Y. Chen, Reaction evolution and alternative layer formation in $Sn/(Bi_{0.25}Sb_{0.75})_2Te_3$ and Sn/Sb_2Te_3 couples, J. Alloys Comp. 553 (2013) 106-112.

[16] P.E.J. Flewitt and R.K. Wild, Physical methods for materials characterization, Bristol and Philadelphia: Institute of Physics Publishing, UK, 1994.

[17] T.B. Massalski, H. Okamoto, P.R. Subramanian and L. Kacprzak, Binary Alloy Phase Diagrams, 2nd ed., Vol. 1, in: T.B. Massalski et al., ASM International, Materials Park, OH, 1990, pp. 790-792.

[18] E.A. Brandes and G.B. Brook, Smithells Metals Reference Book, 7th ed., Butterworth-Heinemann, Oxford, 1992.

[19] T.B. Massalski, H. Okamoto, P.R. Subramanian and L. Kacprzak, Binary Alloy Phase Diagrams, 2nd ed., Vol. 1, in: T.B. Massalski et al., ASM International, Materials Park, OH, 1990, pp.3342-3343.

[20] S.-W. Chen, H.-J. Wu, W.-T. Chiu and C.-Y. Wu, unpublished results (2013).

[21] H. Okamoto, The Bi-Se (Bismuth-Selenium) System., J. Phase Equilib. 15 (2) (1994) 195-201.

[22] T.B. Massalski, H. Okamoto, P.R. Subramanian and L. Kacprzak, Binary Alloy Phase Diagrams, 2nd ed., Vol. 1, in: T.B. Massalski et al., ASM International, Materials Park, OH, 1990, pp.800-801.

[23] F. Hulliger, Structural Chemistry of Layer-Type Phases, Springer, Netherlands, 1977.

[24] J.W.G. Bos, H.W. Zandbergen, M.-H. Lee, N.P. Ong and R. J. Cava, The Structures and Thermoelectric Properties of the Infinitely Adaptive Series $(Bi_2)_m(Bi_2Te_3)_n$, Phys. Rev. B 75 (2007) 195203.

Figure captions

Figure 1: BEI micrograph of the Sn/Bi_2Te_3 couple reacted at 250℃ for (a) 5 minutes, (b) 10 minutes and (c) 15 minutes.

Figure 2: (a) Elemental mapping of the reaction zone in the Sn/Bi_2Te_3 couple reacted at 250℃ for 10 minutes. (b) SEI micrograph of the deep-etched reaction zone in the Sn/Bi_2Te_3 couple reacted at 250℃ for 10 minutes using $(CH_3OH)_{93}(HCl)_2(HNO_3)_5$ etchant. (c) Schematic illustration of the mechanism of the entrapped pieces of unreacted Bi_2Te_3.

Figure 3: The reaction layer thickness in the Sn/Te [8], Sn/Bi_2Te_3, Sn/Bi_2Se_3, Sn/Sb_2Te_3 [15], $Sn/(Bi_{0.25}Sb_{0.75})_2Te_3$ [15] and $Sn/Bi_2(Te_{1-x}Se_x)_3$ couples reacted at 250℃. The Y-axis on the right is for Sn/Te, Sn/Bi_2Te_3, Sn/Sb_2Te_3 and $Sn/(Bi_{0.25}Sb_{0.75})_2Te_3$ and that on the left is for the Sn/Bi_2Se_3 and $Sn/Bi_2(Te_{1-x}Se_x)_3$.

Figure 4: BEI micrograph of the Sn/Bi_2Se_3 couple reacted at 250℃ for (a) 10 minutes, (b) 30 minutes (c) 60 minutes and (d) 90 minutes.

Figure 5: Elemental mapping of the reaction zone in the Sn/Bi_2Se_3 couple reacted at 250℃ for 90 minutes.

Figure 6: The reaction path in the Sn/Bi_2Se_3 couple superimposed on the Sn-Se-Bi 250℃ phase equilibria isothermal section.

Figure 7: BEI micrograph of the $Sn/Bi_2(Te_{0.9}Se_{0.1})_3$ couple reacted at 250℃ for (a) 10 minutes, (b) 30 minutes, (c) 60 minutes, (d) 90 minutes and (e) 120 minutes.

Figure 8: BEI micrograph of the $Sn/Bi_2(Te_{2.9}Se_{0.1})$ couple reacted at 250℃ for (a) 30 minutes, (b) 60 minutes, and (c) 90 minutes.

Figure 1(a) TIF

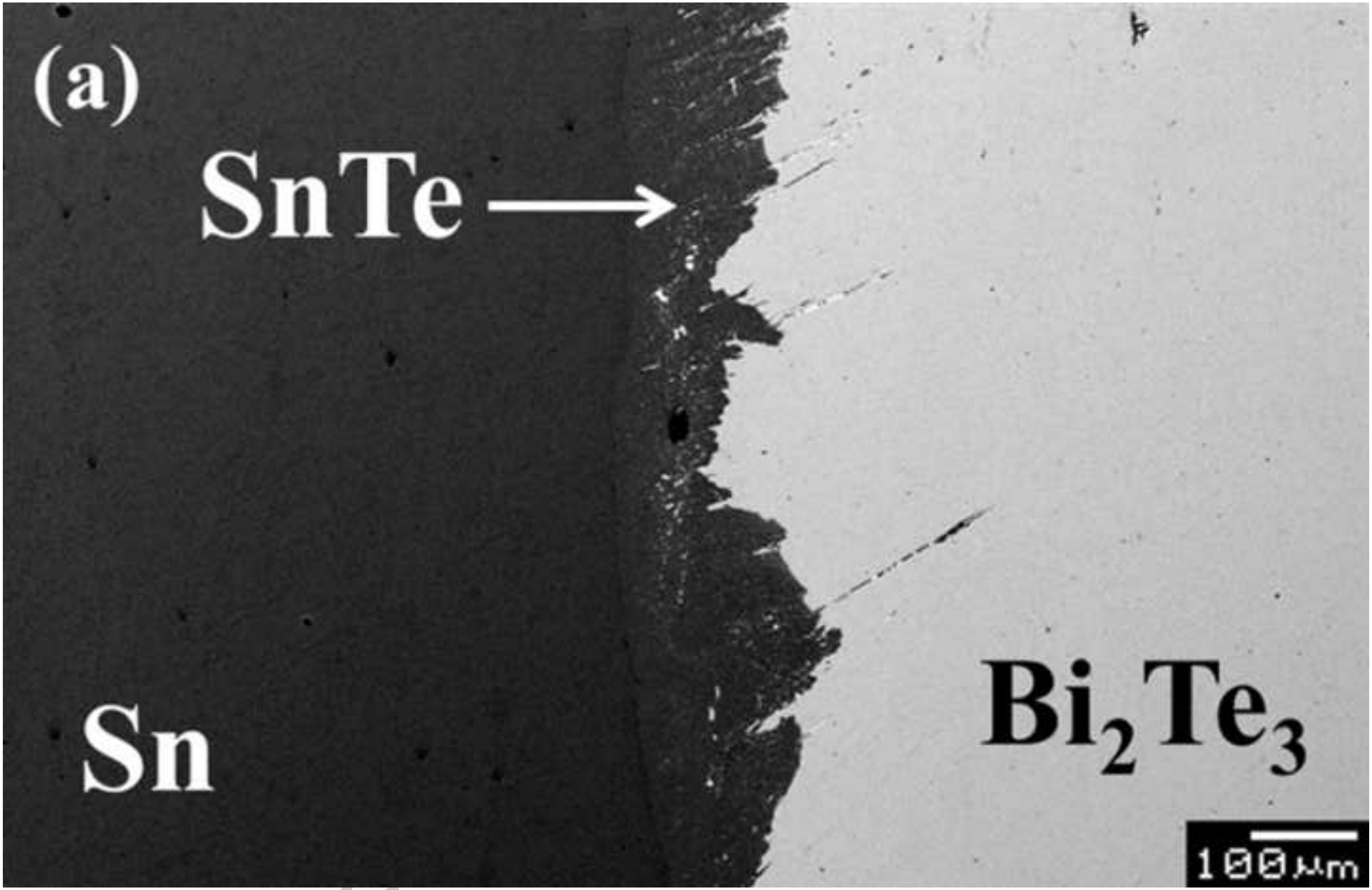

Figure 1(b) TIF

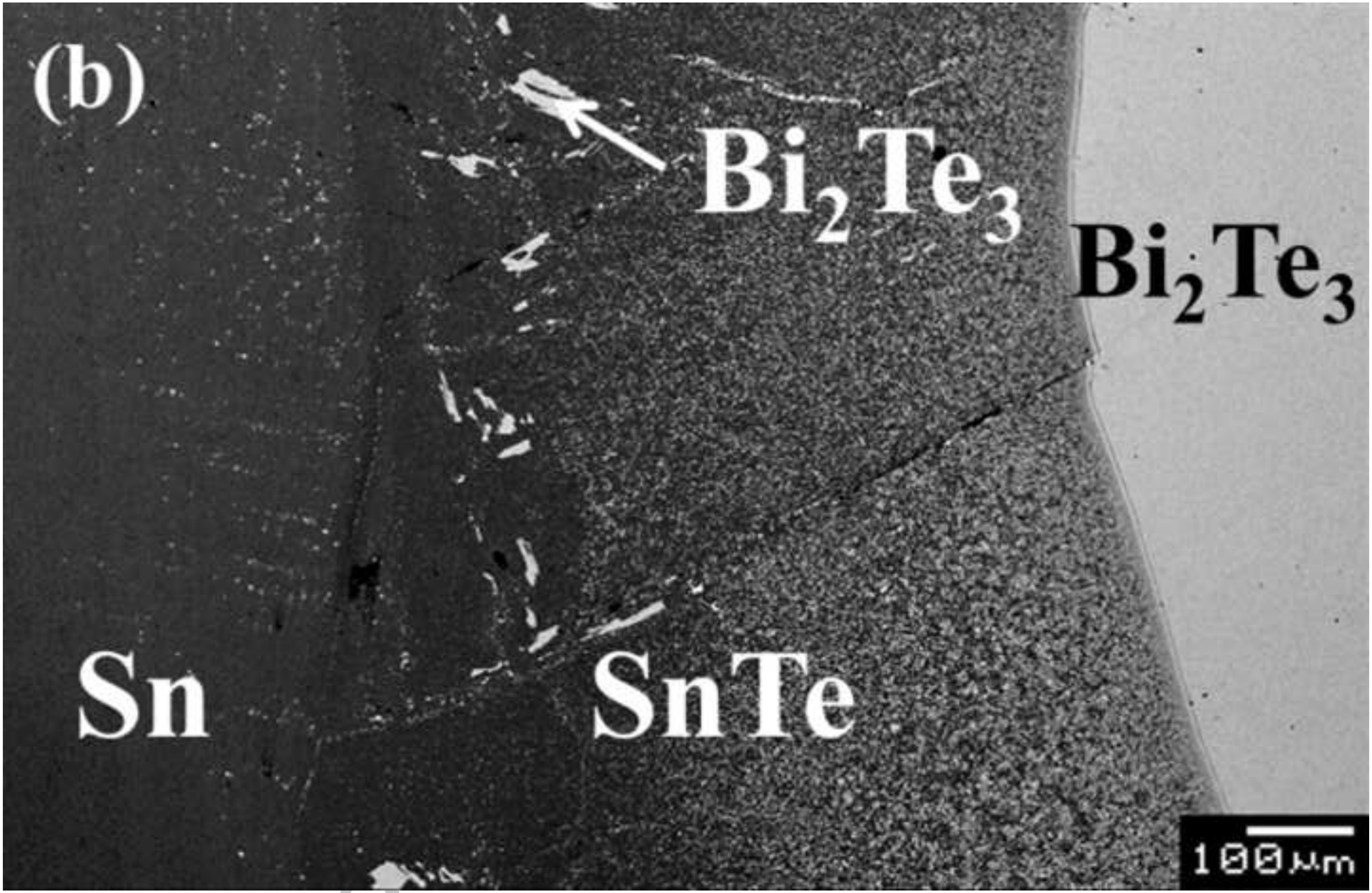

Figure 1(c) TIF

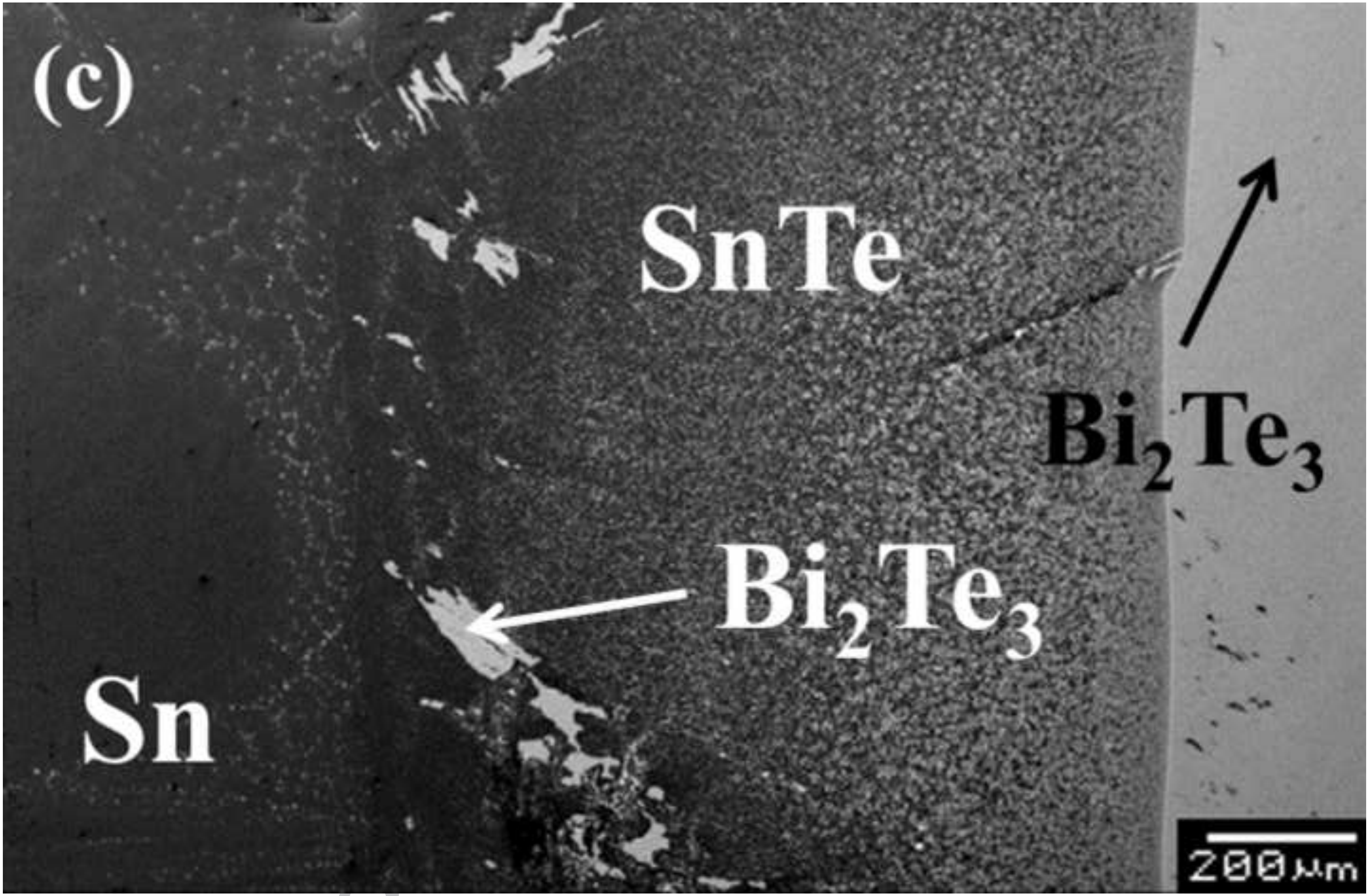

Figure 2(a) TIF

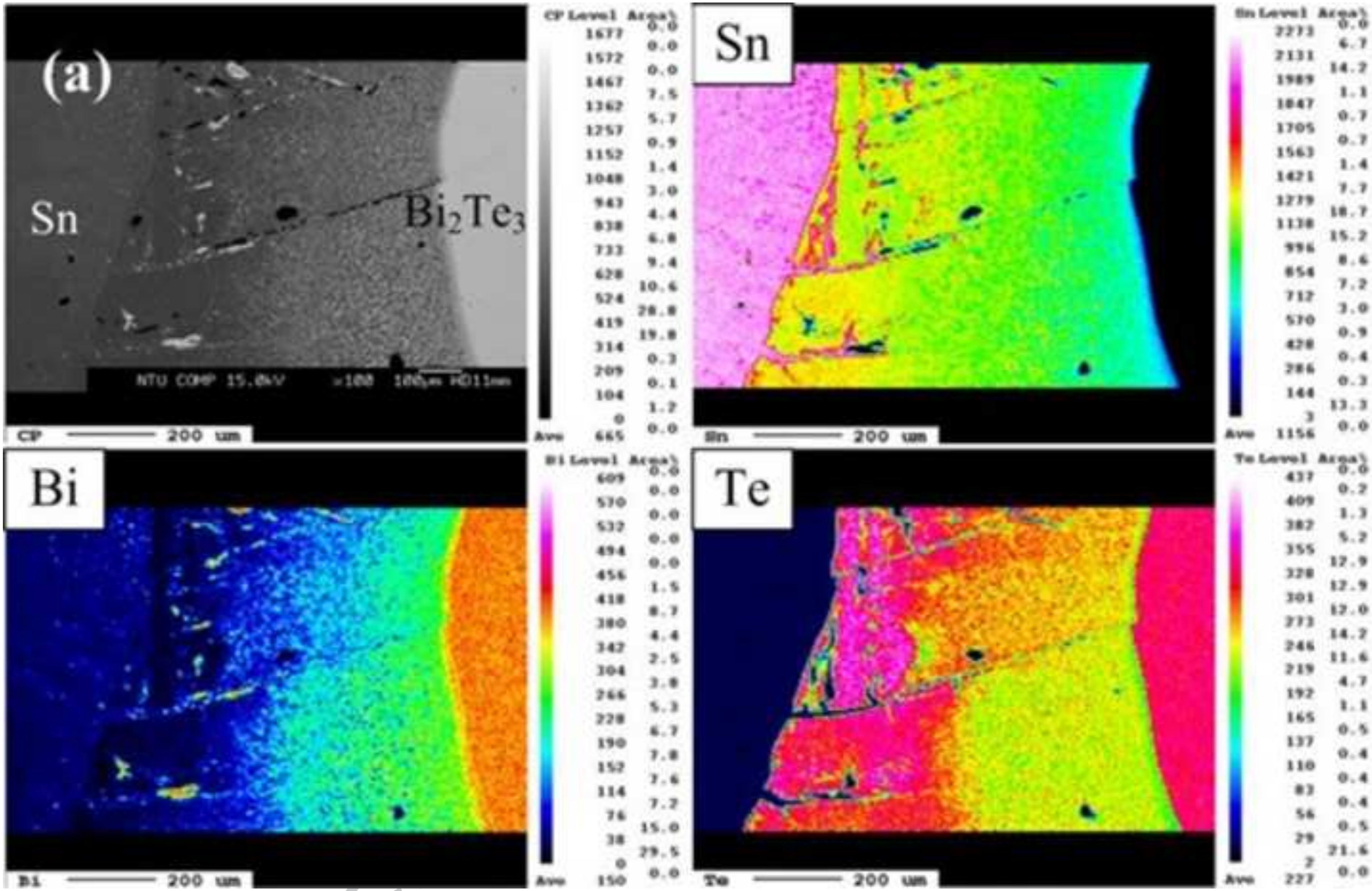

Figure 2(b) TIF

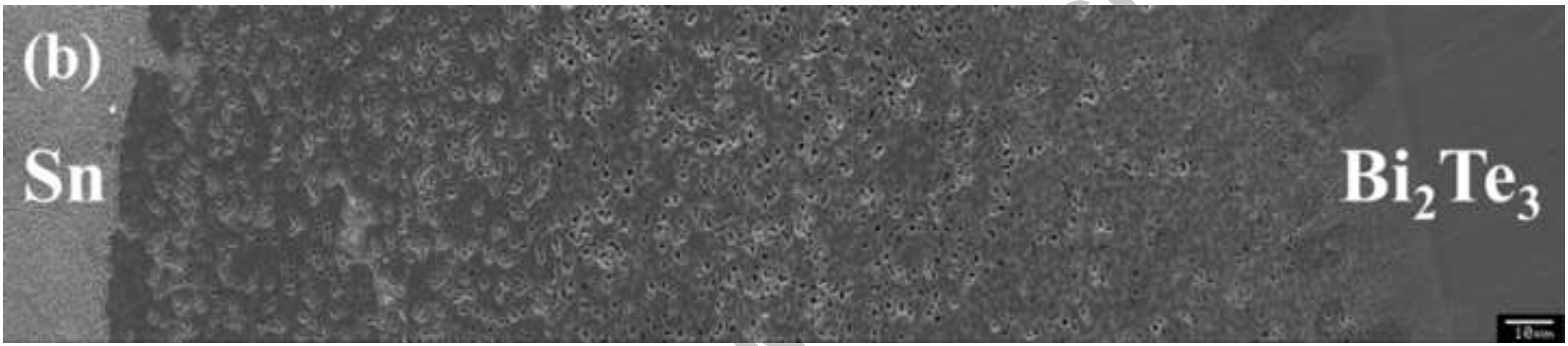

Figure 2(c) TIF

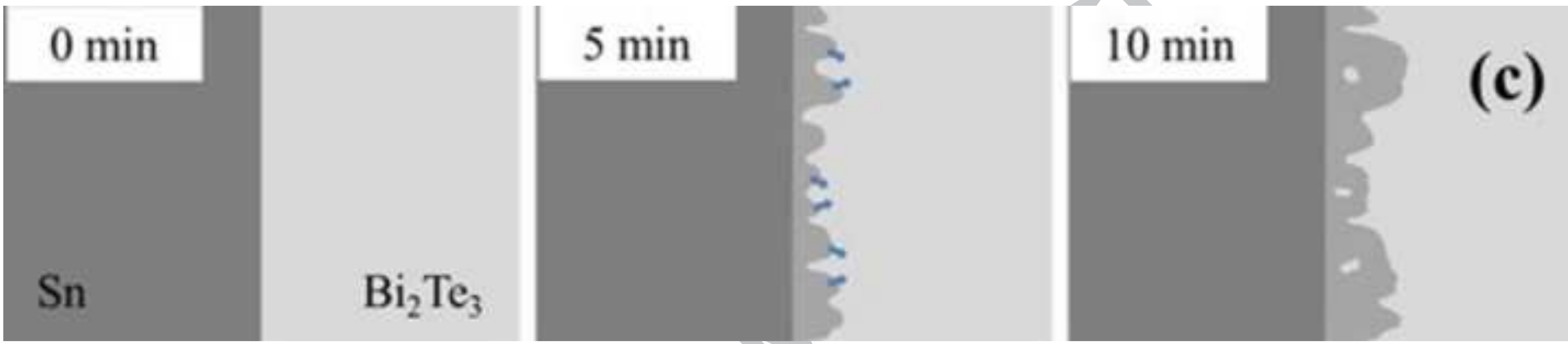

Figure 3 TIF

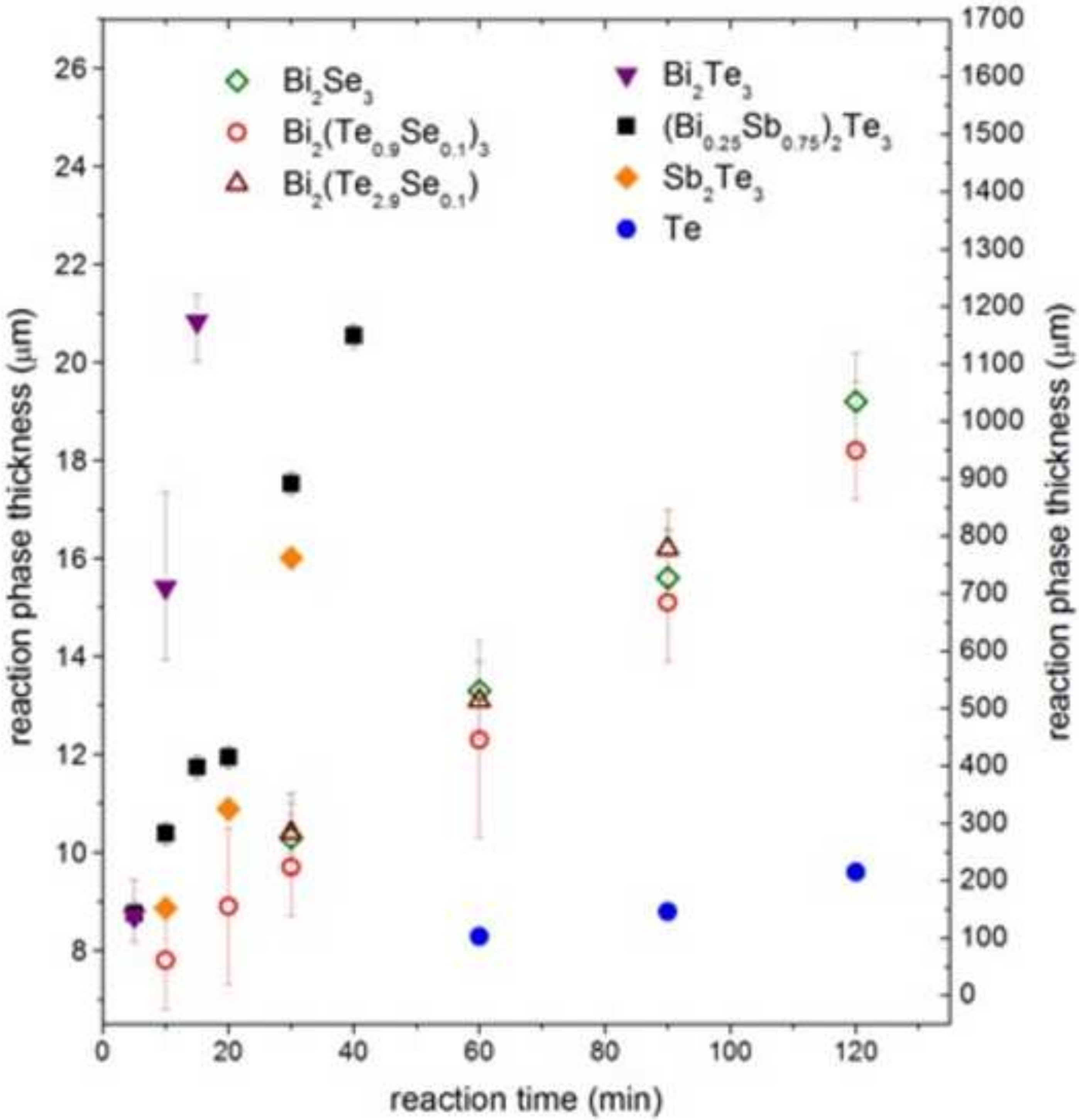

Bi_2Se_3
$Bi_2(Te_{0.9}Se_{0.1})_3$
$Bi_2(Te_{2.9}Se_{0.1})$
Bi_2Te_3
$(Bi_{0.25}Sb_{0.75})_2Te_3$
Sb_2Te_3
Te
reaction phase thickness (μm)
reaction phase thickness (μm)
reaction time (min)
0
20
40
60
80
100
120
8
10
12
14
16
18
20
22
24
26
0
100
200
300
400
500
600
700
800
900
1000
1100
1200
1300
1400
1500
1600
1700

Figure 4(a) TIF

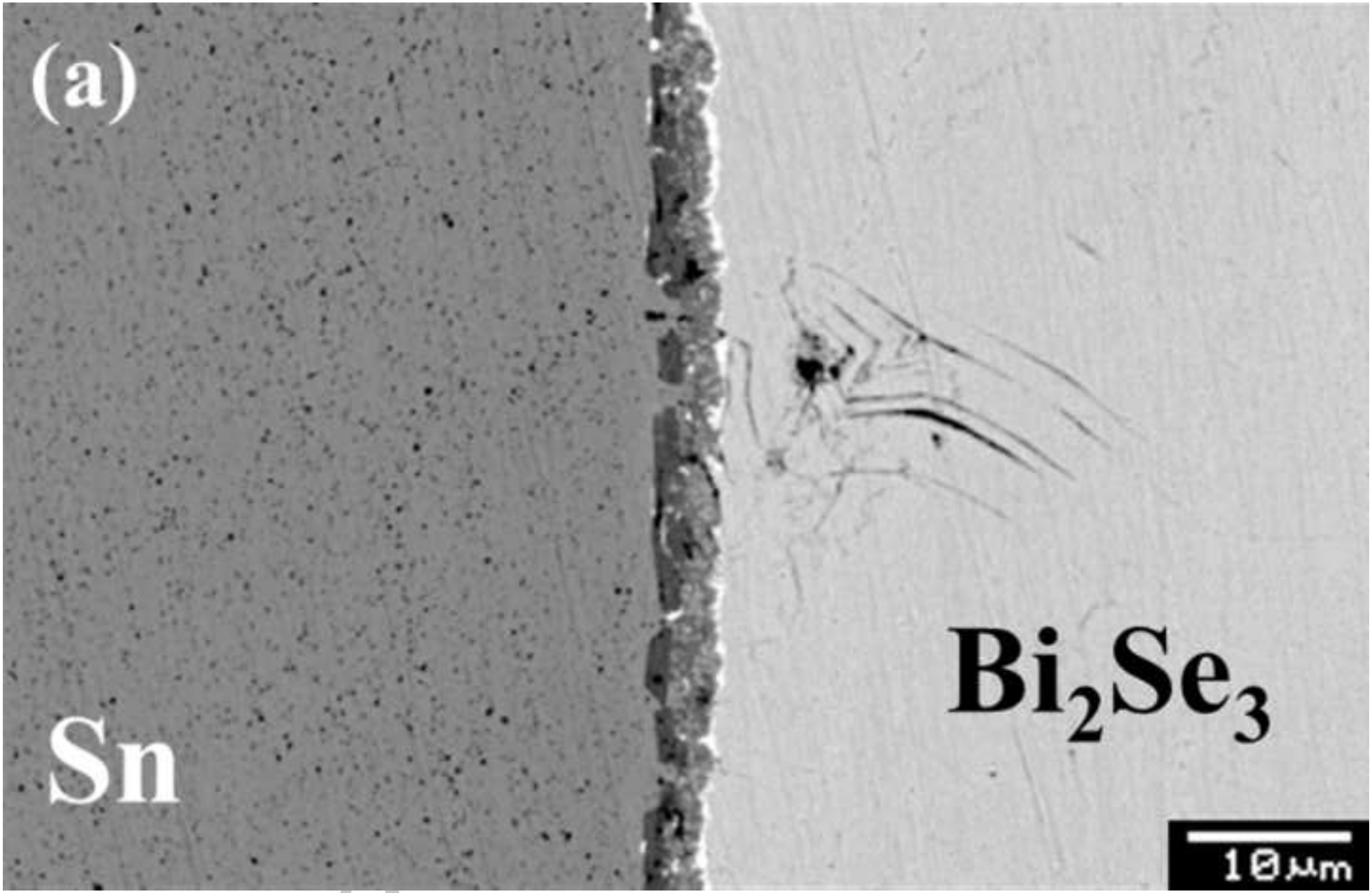

Figure 4(b) TIF

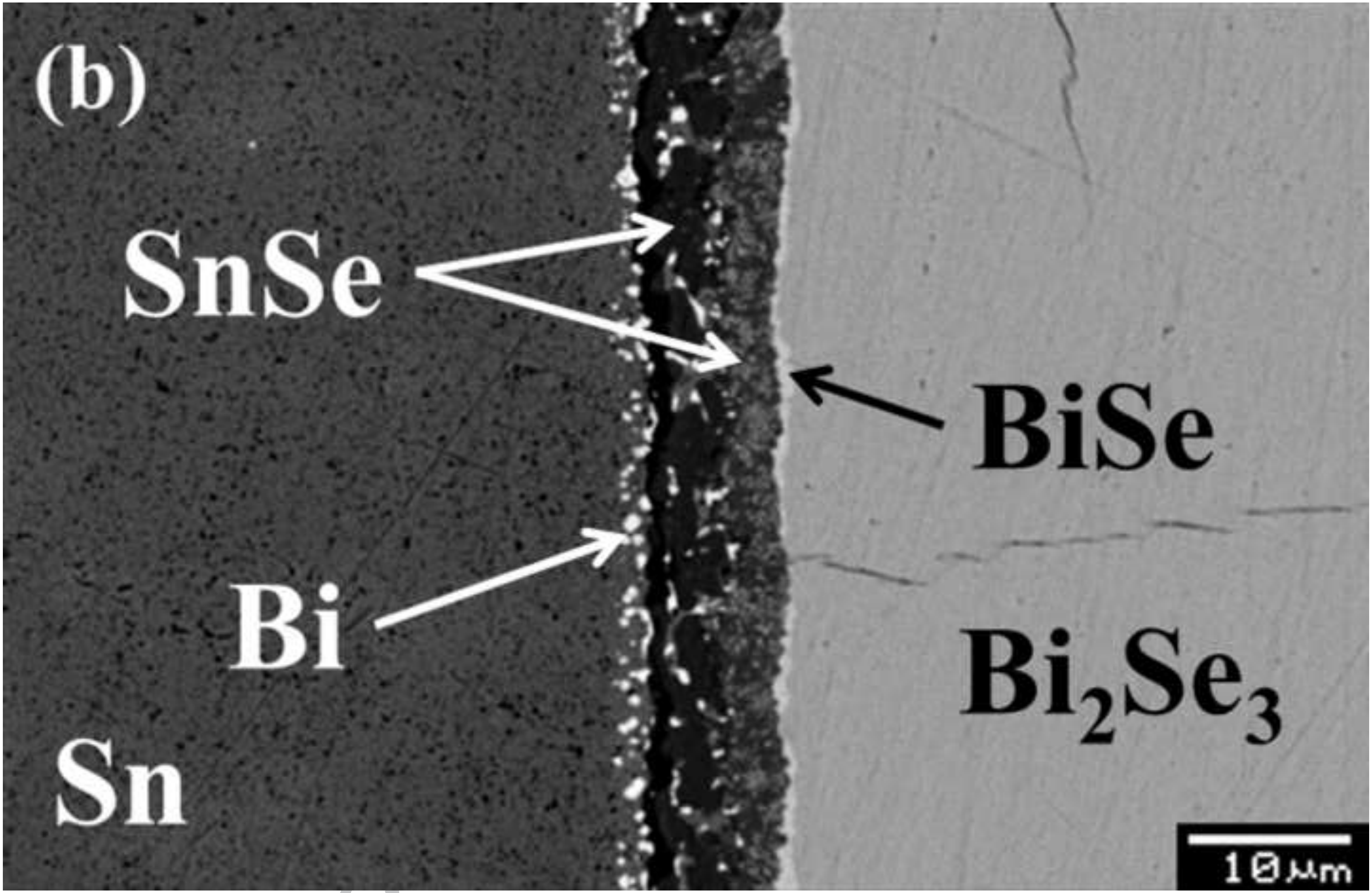

Figure 4(c) TIF

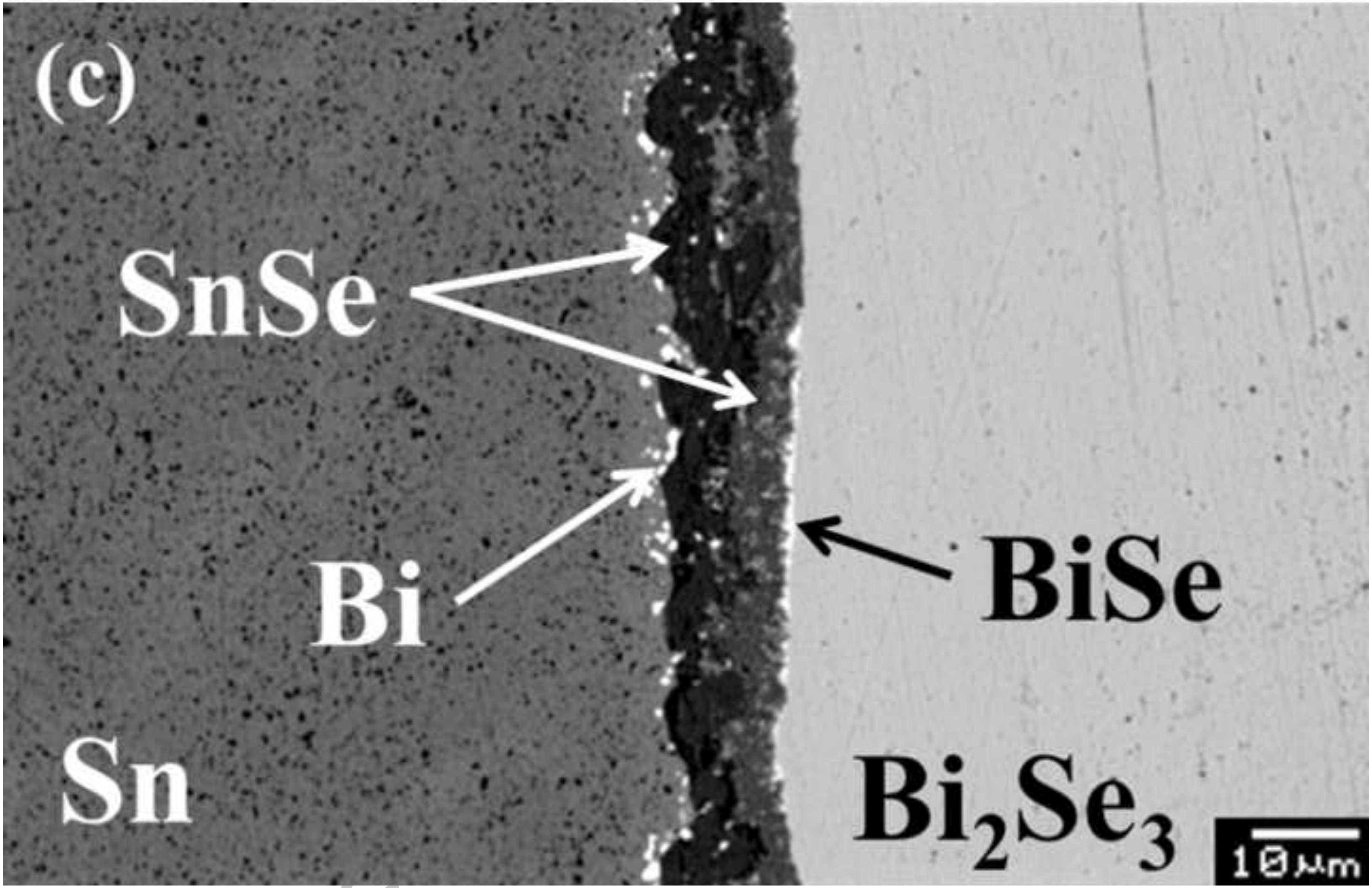

Figure 4(d) TIF

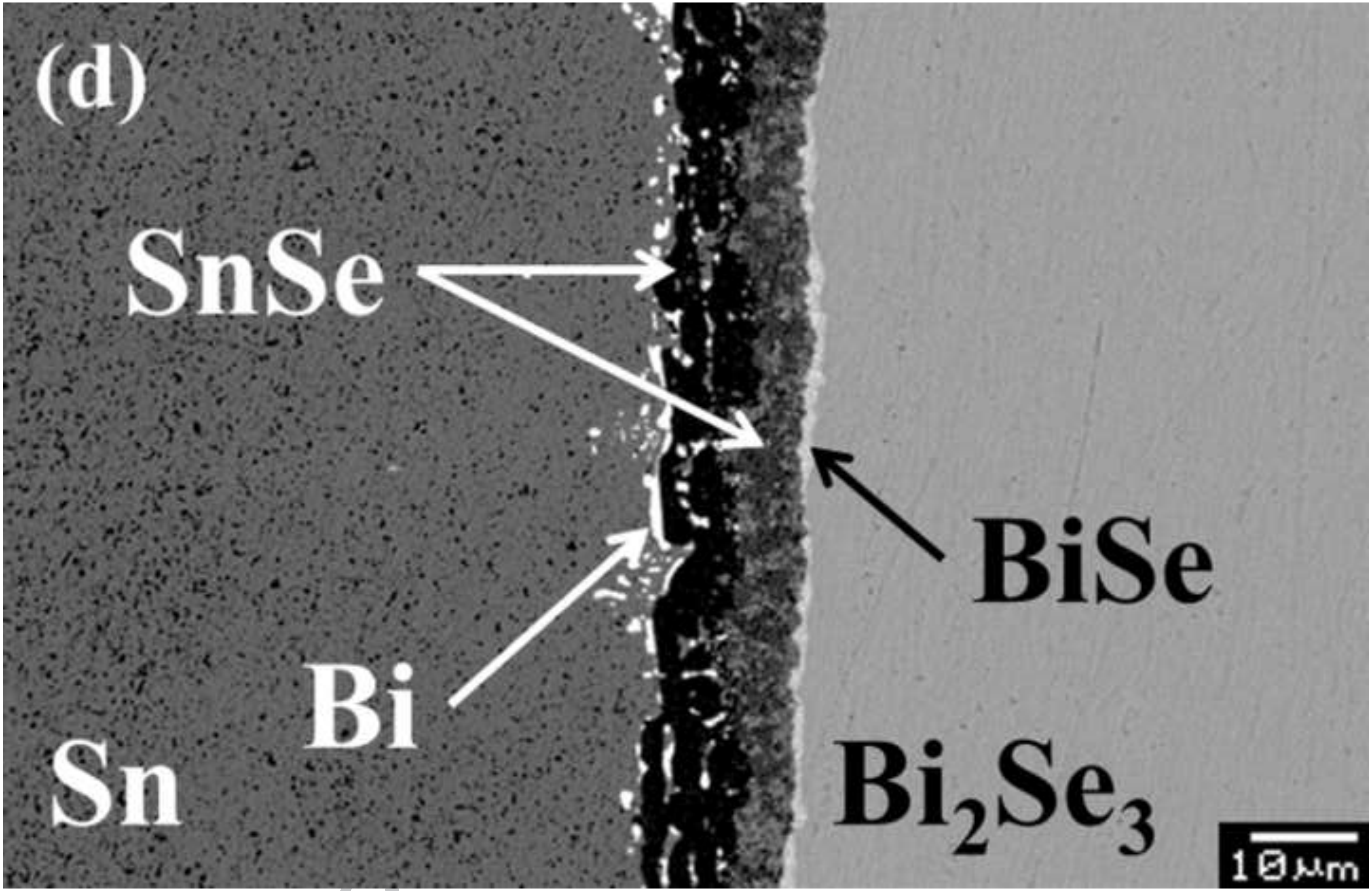

Figure 5 TIF

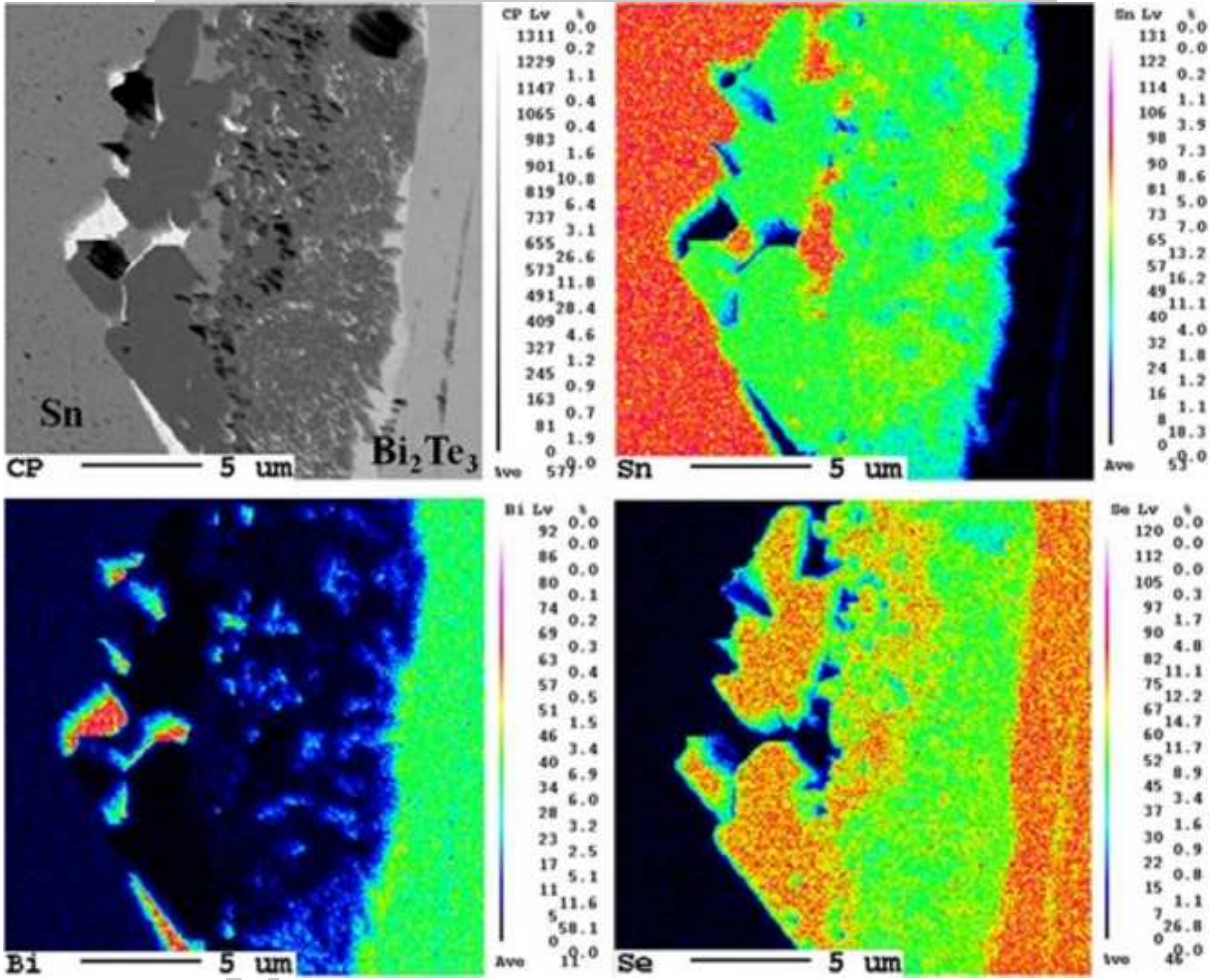

Figure 6 TIF

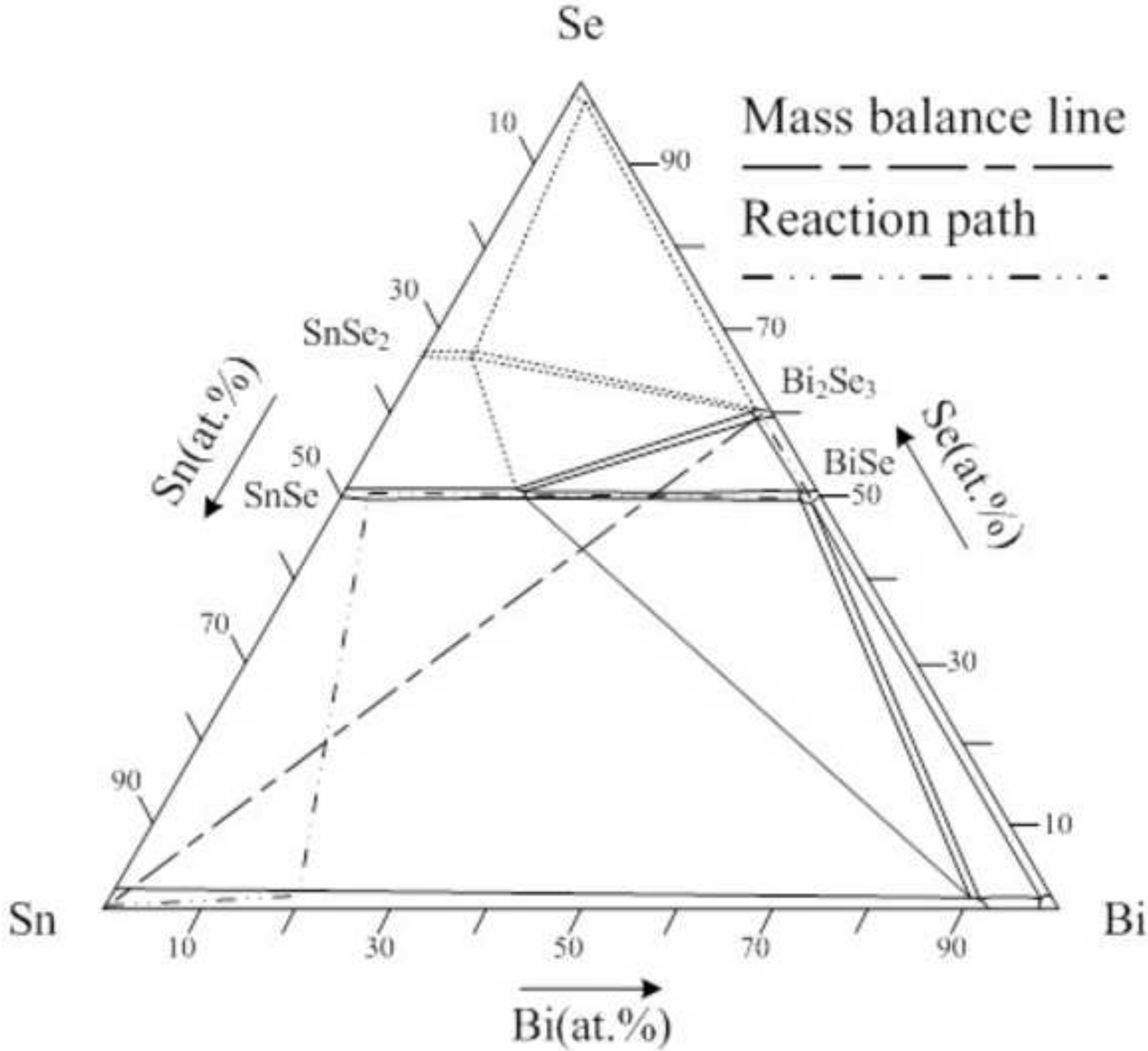

Se
Mass balance line
Reaction path
SnSe₂
Bi₂Se₃
BiSe
SnSe
Sn(at.%)
Se(at.%)
Sn
Bi
Bi(at.%)
10
30
50
70
90

Figure 7(a) TIF

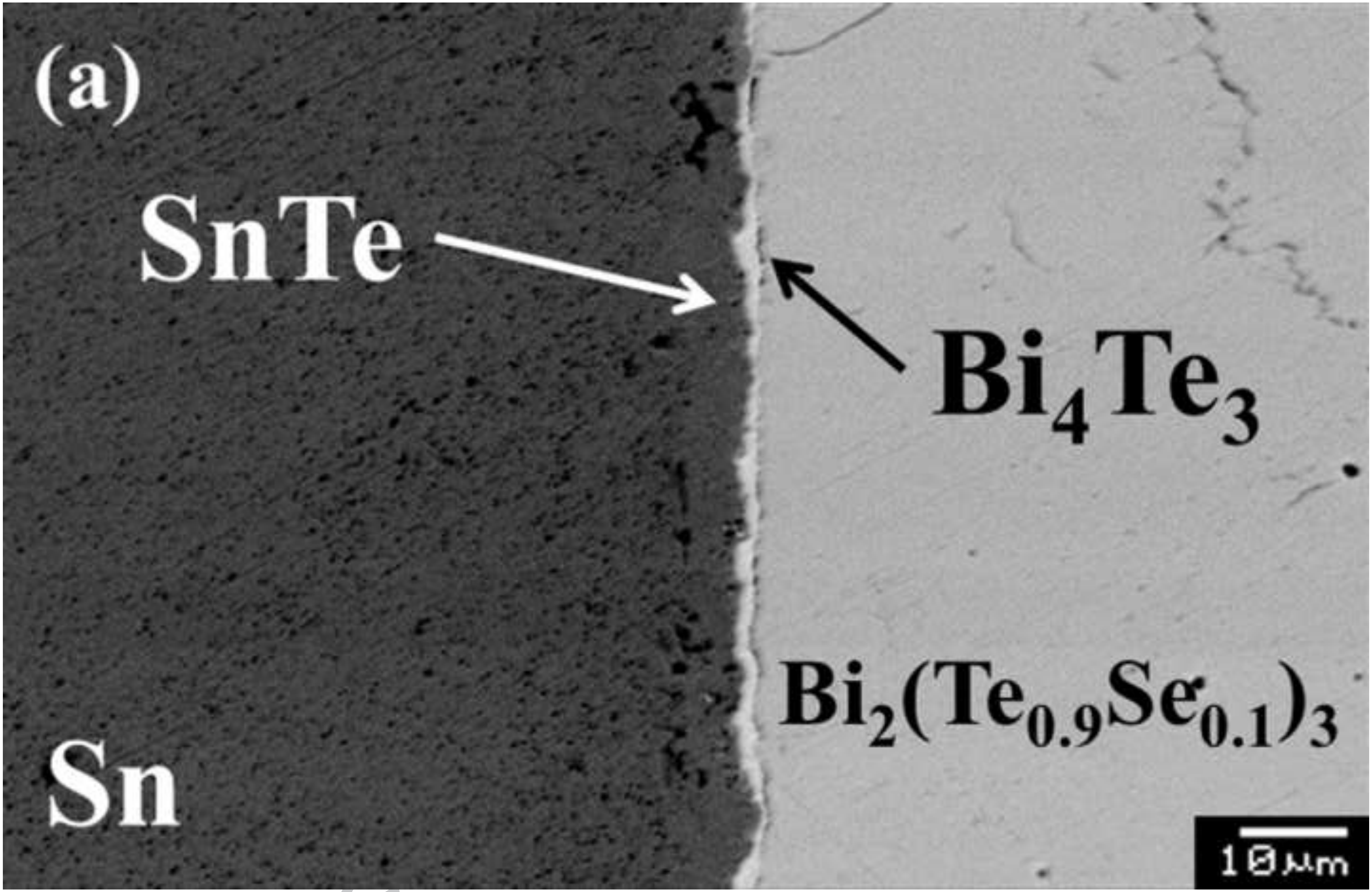

Figure 7(b) TIF

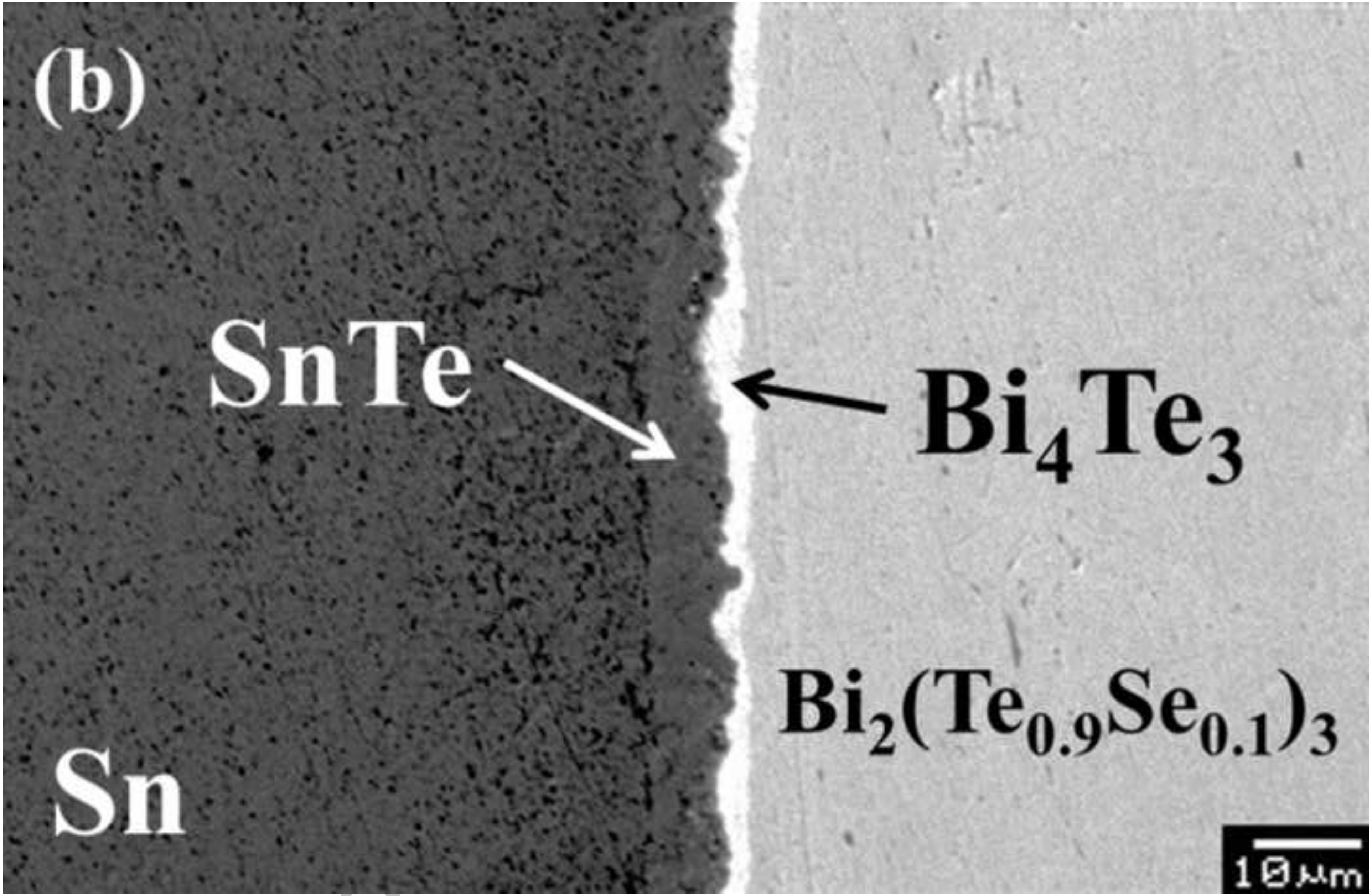

Figure 7(c) TIF

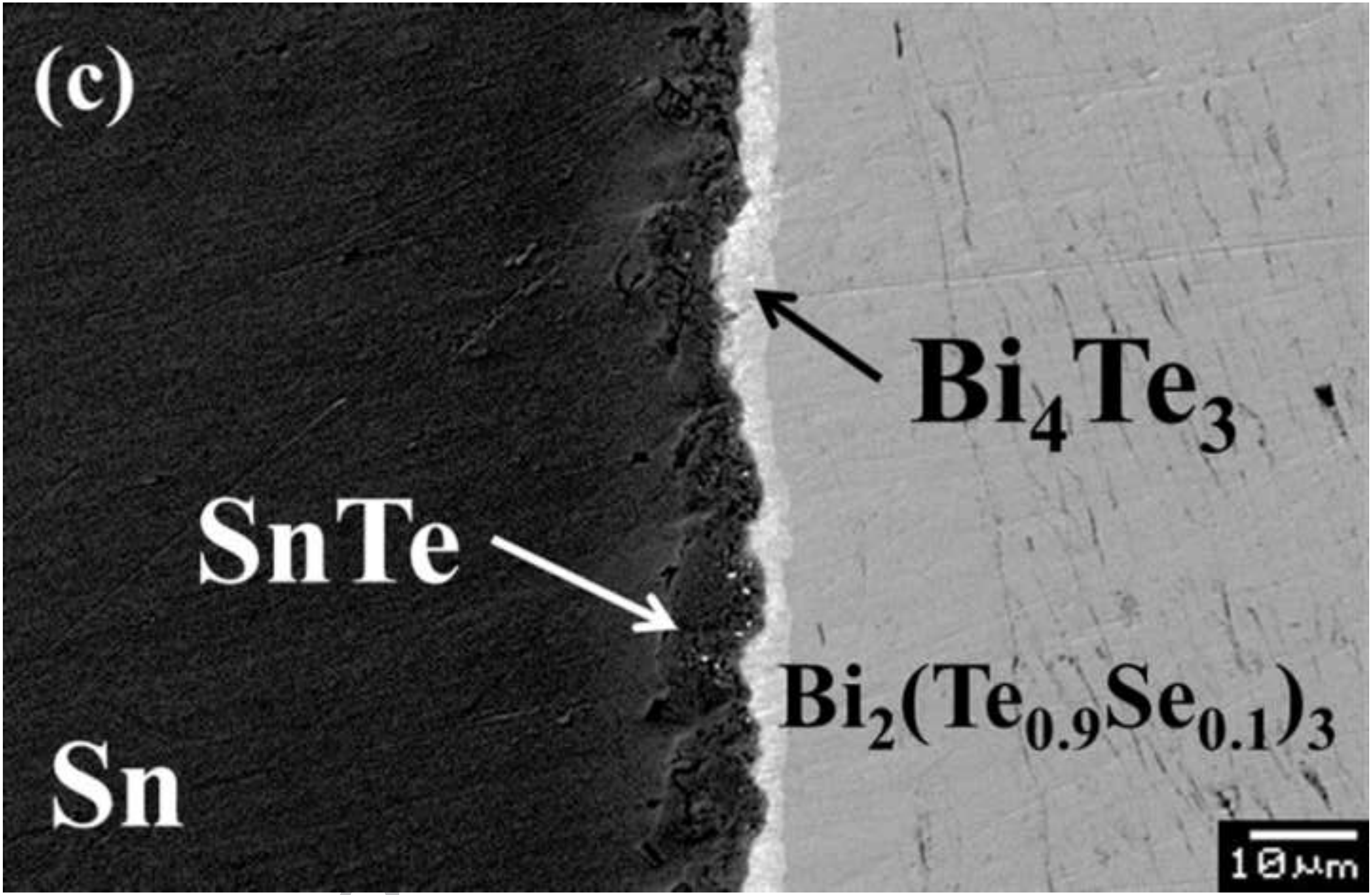

Figure 7(d) TIF

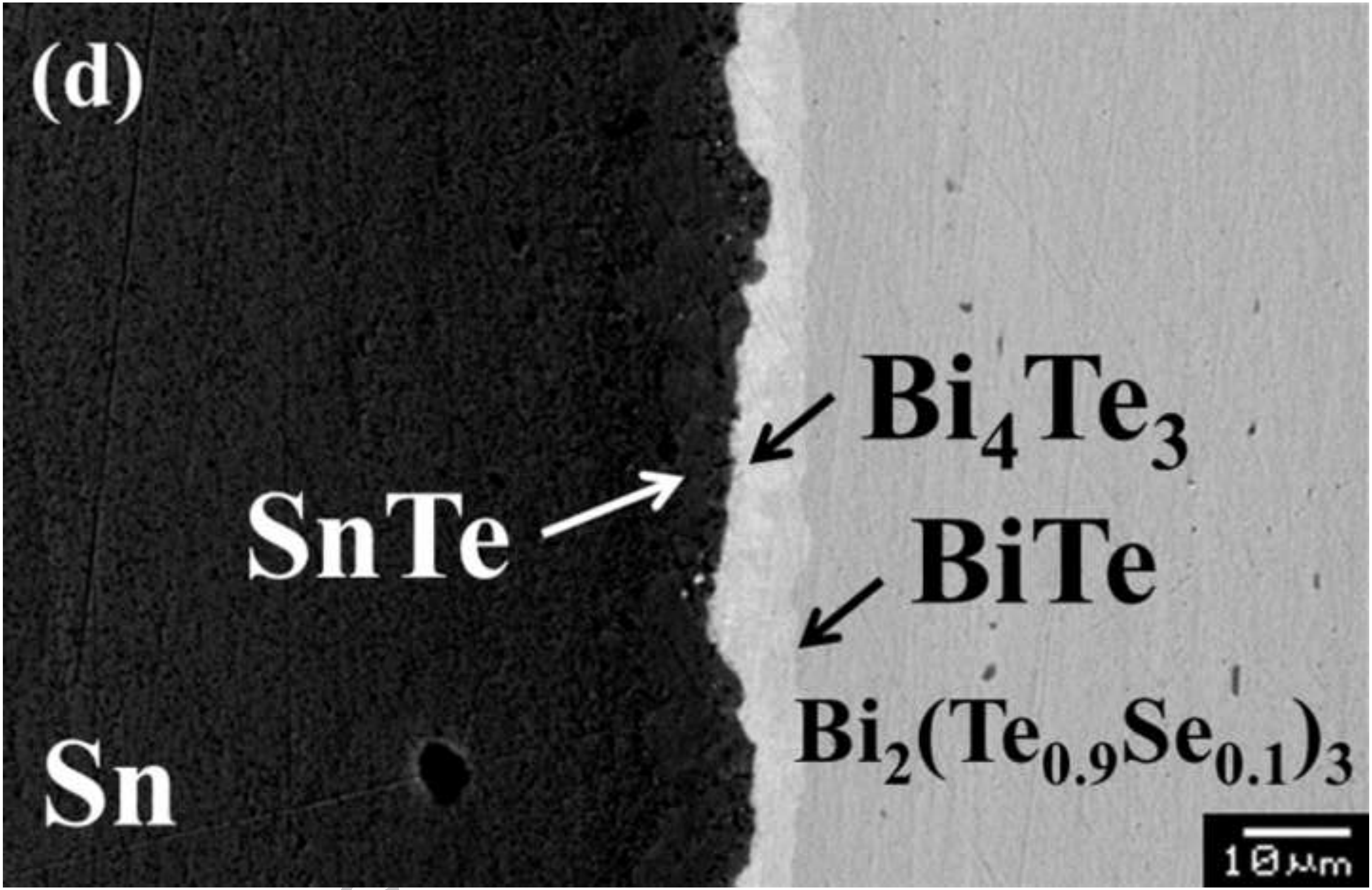

Figure 7(e) TIF

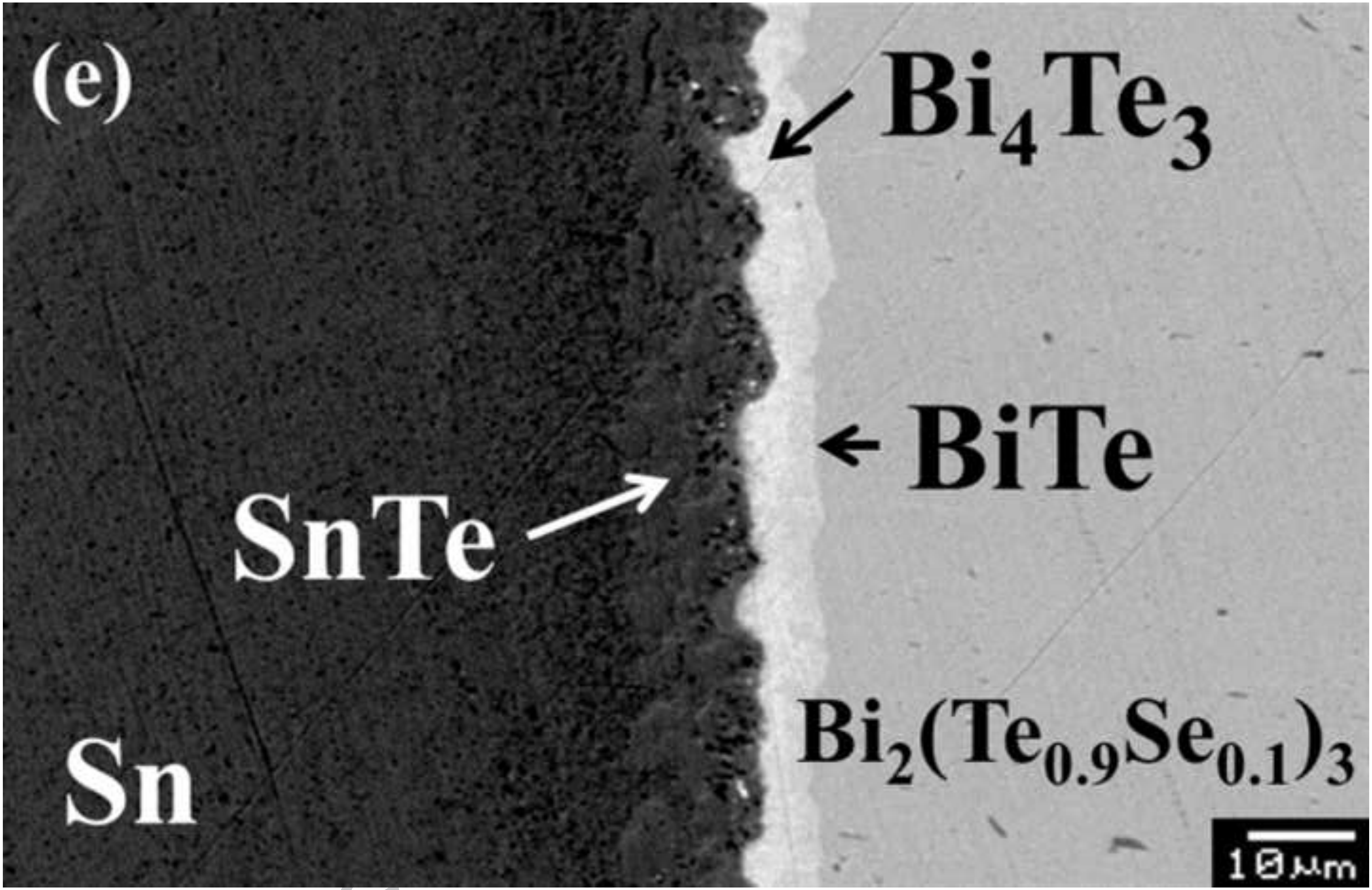

Figure 8(a) TIF

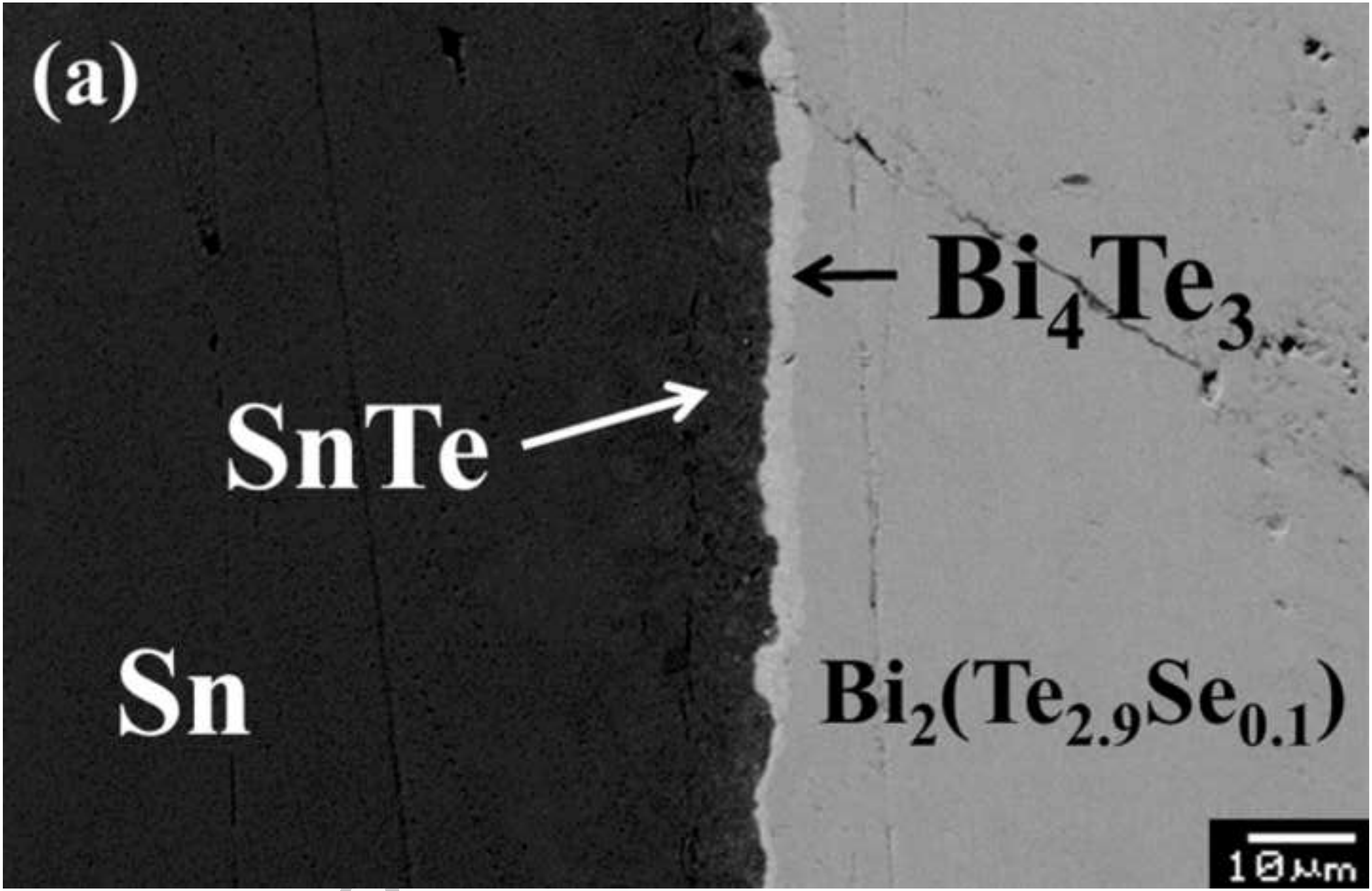

Figure 8(b) TIF

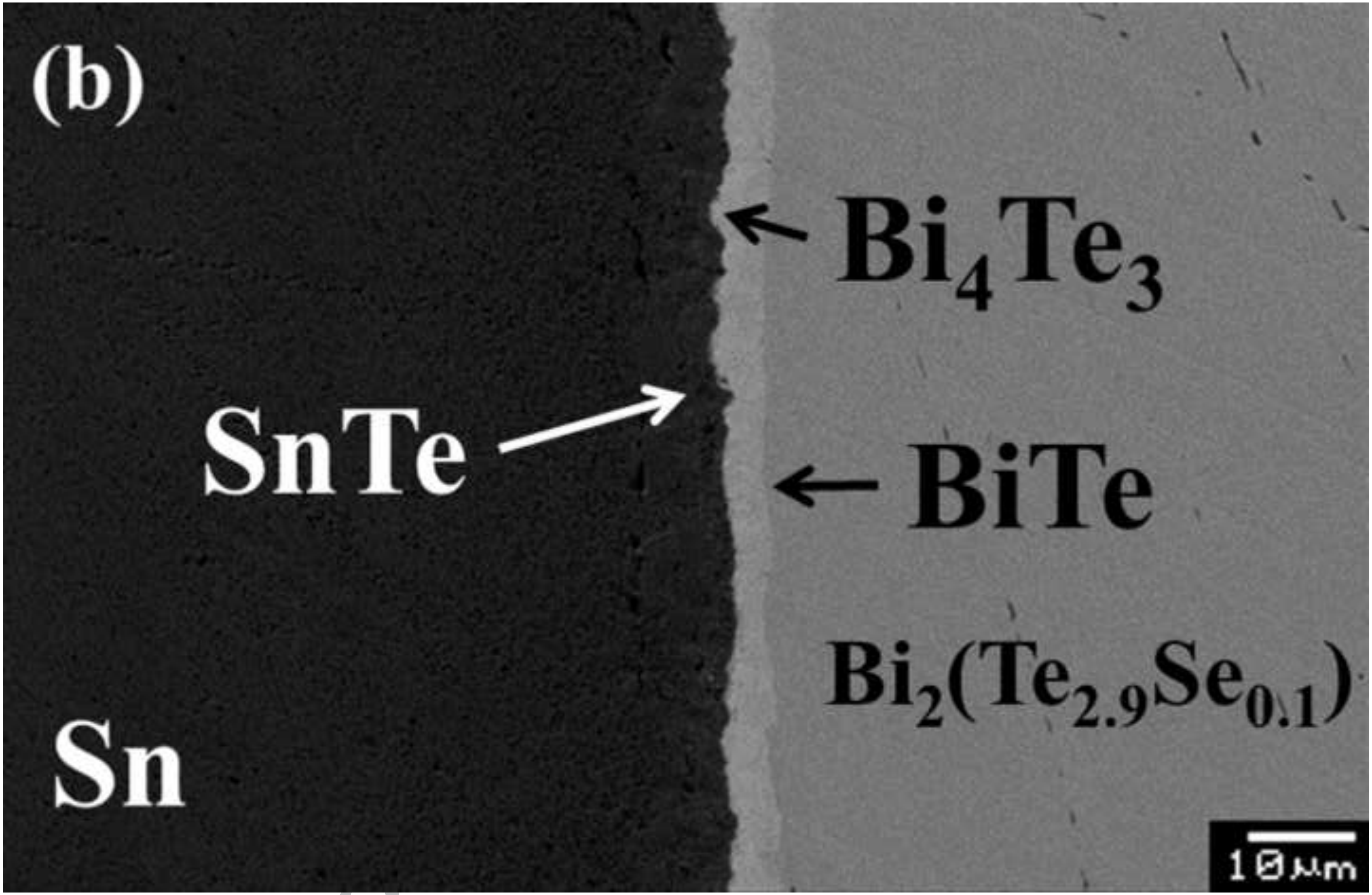

Figure 8(c) TIF

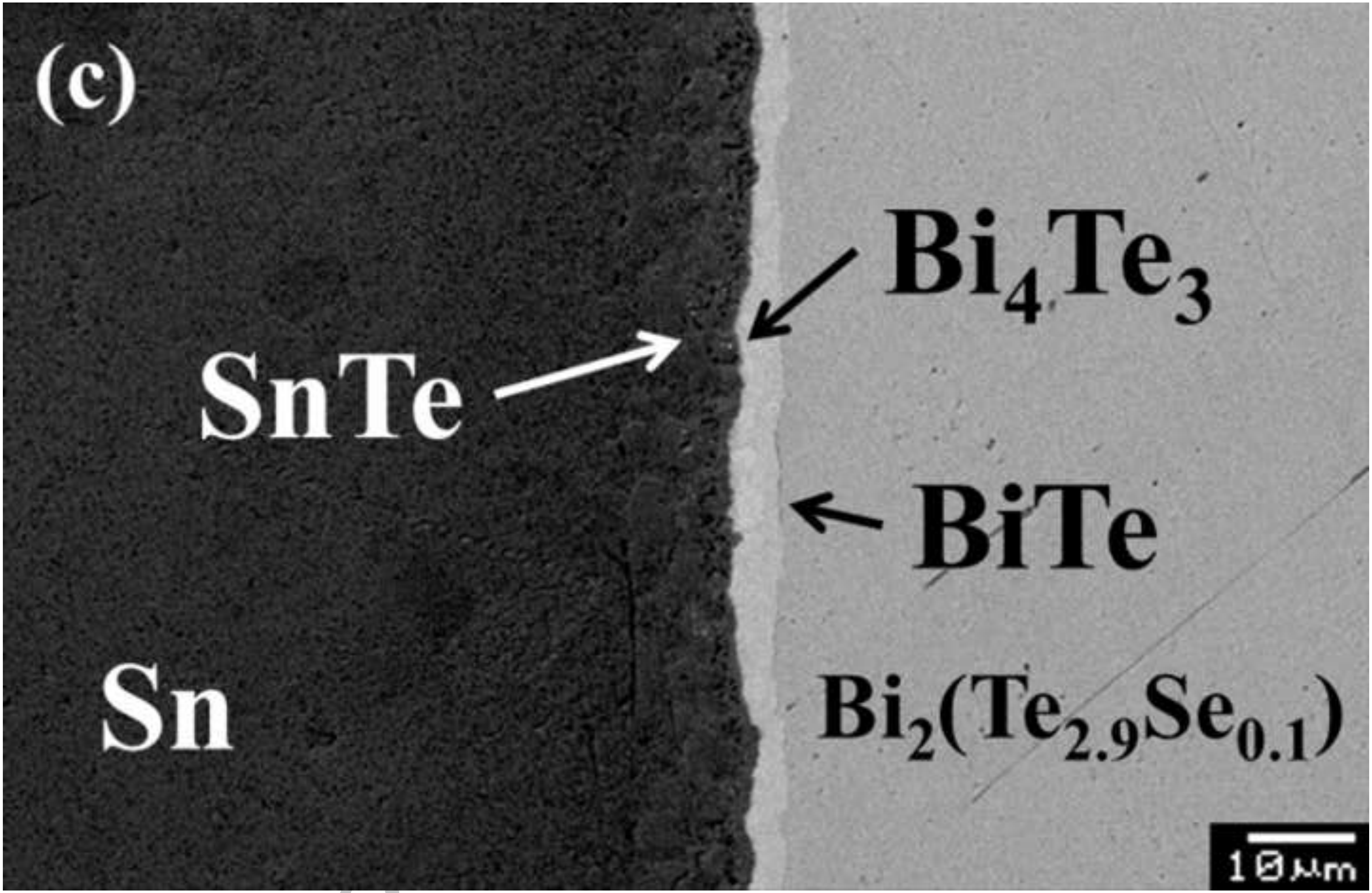

Highlights

國立清華大學 化學工程學系

National Tsing Hua University

Department of Chemical Engineering

#101, Sec. 2, Kuang-Fu Road, Hsinchu, Taiwan 300

Tel: (03)5721734, Fax: (03)5715408

- Interfacial reactions in the $Sn/Bi_2(Te_{1-x}Se_x)_3$ couples are examined at 250°C
- The reaction paths in the $Sn/Bi_2(Te_{1-x}Se_x)_3$ couples are determined.
- The reaction layer is 1174 μm in $Sn/B_{i2}Te_3$ after reaction for 15 minutes.
- The reaction rates are changed dramatically with only 2.0at%Se addition to Bi_2Te_3.
- The layer is less than 9 μm in $Sn/Bi_2(Te_{2.9}Se_{0.1})_3$ after reaction for 15 minutes.

Graphical Abstract